Quantum Electronics **37** (11) 1015 – 1020 (2007)

NONLINEAR OPTICAL PHENOMENA

PACS numbers: 42.65.Re; 32.80.Rn; 42.62.Eh
DOI: 10.1070/QE2007v037n11ABEH013492

Low- and high-frequency continuum generation by femtosecond pulses in fused silica

A.P. Sukhorukov, N.Yu. Vislobokov

***Abstract*. The dynamics of continuum generation by a superpower ultrashort pulse in fused silica is numerically simulated taking into account photon ionisation. It is found that a high-intensity femtosecond laser pulse splits during its propagation into subpulses and subbeams. The emission spectrum is shown to broaden considerably both to the high- and low-frequency regions.**

Keywords: *femtosecond pulse, supercontinuum, ionisation, multiphoton ionisation, tunnelling, avalanche plasma formation.*

1. Introduction

The development of laser systems for generating terawatt pulses of duration less than 200 fs has inspired a renewed interest in the problem of supercontinuum generation in continuous optical media [1]. This phenomenon has been observed for the first time by Alfano and Shapiro as early as 1970 [2] upon focusing high-power picosecond pulses in gas; later, it was observed by many researchers in gases, liquids, and solids [3 – 8].

Of special interest is supercontinuum generation in widespread transparent dielectrics such as sapphire and fused silica. Such a broadband laser emission can be used in spectroscopy [9, 10], in devices for pulse compression [11], fibre optics [12], optical coherence tomography, metrology, etc.

It is known that spectra can be broadened due to self-phase modulation, four-wave mixing, increasing the steepness of laser pulses during their propagation, and ionisation processes. It has been found in [3, 4, 7, 9] that supercontinuum generation by high-power femtosecond pulses in a continuous transparent medium occurs due to the self-phase modulation of the light field and the appearance of its temporal gradient caused by the action of induced photoionisation processes (multiphoton avalanche and tunnelling ionisation) on propagating laser radiation. In particular, supercontinuum generation by picosecond pulses is caused to a considerable extent by the avalanche formation of the electron plasma. This severely complicates the application of nonlinear dielectrics as sources of broadband optical emission because the density of the free electron plasma (FEP) after the formation of an electron avalanche drastically increases up to critical values at which a dielectric is damaged. At the same time, during the propagation of a femtosecond laser pulse in a dielectric, an electron avalanche has no time to develop due to the short pulse duration. The plasma is predominantly produced due to multiphoton and tunnelling ionisation, and therefore a continuum can be generated at the FEP density lower than the critical value, when no structural changes occur in the dielectric crystal [1, 4 – 7].

Note that the spectrum in transparent dielectrics not always broadens both to the high- and low-frequency regions. For example, upon continuum generation, the pedestal of the spectrum broadens, as a rule, to the high-frequency region and almost does not broaden to the low-frequency region [1, 5, 7, 8, 12]. By analogy with a number of modern papers in this field, if the emission spectrum broadens considerably only to the high-frequency region or only to the low-frequency region, we are dealing with the generation of a continuum, and if the emission spectrum noticeably broadens both to the high- and low-frequency regions, a supercontinuum is generated.

We selected a dielectric for a numerical study due to the known advantages of solids from the point of view of continuum generation. For example, it was found in experiments [1] that the band gap of a dielectric limits the possibility of supercontinuum generation. A considerable broadening of the spectrum in experiments on supercontinuum generation in various liquids and solids [1] was observed only in media with the band gap $U \geqslant 4.7$e V. The width of the spectrum generated in materials with greater values of U slightly increased but the minimal power of supercontinuum generation was considerably higher. Fused silica has a broad energy gap for a transparent dielectric ($U = 9$ eV) and at the same time is a widespread and low-cost material. It is possible to generate in it a continuum with a low divergence [4 – 7]. A nonlinear mechanism induced by a pulse causes the quasi-waveguide propagation of a 'white' radiation beam in the medium [1]. Therefore, it seems that fused silica can become a promising material for supercontinuum generation.

The main disadvantage of continuum spectra already observed in fused silica is their strong asymmetry: the spectrum is strongly broadened to the high-frequency region, whereas the broadening to the low-frequency region is almost absent [1, 5, 7, 8, 12].

A.P. Sukhorukov, N.Yu. Vislobokov Department of Physics, M.V. Lomonosov Moscow State University, Vorob'evy gory, 119992 Moscow, Russia; e-mail: apsmsu@gmail.com, nkt_2002@mail.ru

Received 14 December 2006; revision received 14 March 2007
Kvantovaya Elektronika **37** (11) 1015 – 1020 (2007)
Translated by M.N. Sapozhnikov

In this paper, we studied supercontinuum generation by a superpower femtosecond laser pulse in fused silica and analysed the physical nature of this phenomenon. The broadening of the spectrum both to the high- and low-frequency regions can be achieved due to a drastic phase change after the decomposition of the laser pulse into subpulses caused by photoionisation.

2. Physical model

The evolution of a high-power ultrashort laser pulse ($P_{in}/P_{cr} > 1$, where P_{in} is the initial pulse power and P_{cr} is the critical self-focusing power) is mainly caused by the action of two permanently competing processes: self-focusing caused by the nonlinearity of a dielectric and defocusing in the electron plasma. Quite challenging for the study and at the same time very interesting is the case of dynamic competition between these two effects, when the first or second process can alternately dominate during the pulse propagation. The dynamic competition regime is achieved upon irradiation of fused silica by a superpower ultrashort pulse ($P_{in}/P_{cr} > 10$). In this case, the pulse should be short enough to provide the development of an electron avalanche resulting in the optical breakdown of a material. This case is of interest, in particular, because not only the spatiotemporal profile of the pulse but also its spectrum changes noticeably. In addition, the frequency spectrum can broaden considerably both to the high- and low-frequency regions, resulting in supercontinuum generation.

This process can be correctly described by using the modified Schrödinger equation, which takes into account not only diffraction, nonlinearity, and Kerr nonlinearity, but also the fifth-order dispersion and multiphoton, avalanche and tunnel ionisation [13–17].

The field of an ultrashort pulse propagating in a sample is described by the equation

$$\frac{\partial E}{\partial z} = \frac{\mathrm{i}}{2k}\left(\frac{\partial^2}{\partial r^2} + \frac{1}{r}\frac{\partial}{\partial r}\right)\hat{T}^{-1}E - \mathrm{i}\frac{\beta_d}{2}\frac{\partial^2 E}{\partial \tau^2} + P_{nl}, \tag{1}$$

$$P_{nl} = \mathrm{i}k_0 n_2 \hat{T}|E|^2 E + \mathrm{i}k_0 n_4 \hat{T}|E|^4 E - \frac{\sigma_{ibs}}{2}\hat{T}^{-1}(1 + \mathrm{i}\omega_0\tau_c)\rho E - \frac{1}{2}\frac{W_{phi}U}{|E^2|}E, \tag{2}$$

where

$$\hat{T} = \left(1 + \frac{\mathrm{i}}{\omega_0}\frac{\partial}{\partial \tau}\right);$$

E is the electric field strength; z is the longitudinal coordinate; r is the transverse coordinate; $\tau = t - z/v_g$ is the time in the coordinate system moving with the pulse; $v_g = \partial\omega/\partial k|_{\omega_0}$ is the group velocity; $k_0 = n_0\omega/c$ is the wave number; $\beta_d = \partial^2 k/\partial\omega^2|_{\omega_0}$ is the group-velocity dispersion coefficient; n_0 is the linear part of the refractive index; n_2 and n_4 are nonlinearity coefficients of the refractive index; $\sigma_{ibs} = k\omega_0\tau_c/[n_0^2\rho_{cr}(1 + \omega_0^2\tau_c^2)]$ is the cross section of inverse bremsstrahlung absorption of light by electrons (according to the Drude–Stuart model [18]); ω is the frequency; ω_0 is the central laser radiation frequency; τ_c is the characteristic electron collision time; ρ is the free electron density; ρ_{cr} is the critical FEP density; $W_{phi}(|E|)$ is the photon ionisation rate; and U is the band gap of a dielectric.

The model should also take into account a change in the free electron density caused by the action of the field of the propagating pulse. The corresponding evolution equation for the FEP density, taking into account multiphoton ionisation, electron tunnelling from the valence to conduction band (through the band gap of the dielectric) and avalanche ionisation, can be represented in the form

$$\frac{\partial \rho}{\partial t} = W_{phi} + \eta\rho|E|^2 - \frac{\rho}{\tau_r}, \tag{3}$$

where $\eta = \sigma_{ibs}/U$ and τ_r is the relaxation time of the medium. The first term in the right-hand side of (3) describes the contribution of photon ionisation to the generation of free electrons, while the influence of the avalanche formation of the FEP is described by the second term. The third term takes into account the electron recombination.

Let us now calculate W_{phi}. According to the results of recent studies [17], the best fit of the experimental data obtained at superhigh intensities ($I \approx 3.5 \times 10^{13}$ W cm^{-2}), when some physical process interact with each other and at the same time affect a propagating pulse, was achieved by calculating W_{phi} by the method proposed by Keldysh [19]:

$$W_{phi}(|\boldsymbol{E}|) = \frac{2\omega_0}{9\pi}\left(\frac{\omega_0 m^*}{\hbar\sqrt{\Gamma}}\right)^{3/2} Q(\gamma, x)\exp(-\alpha \mathrm{Int}\langle x + 1\rangle),$$

where $\gamma = \omega_0/[e\boldsymbol{E}(m^*U)^{1/2}]$; $m^* = 0.634m_e$ is the effective mass; m_e is the electron mass;

$$\Gamma = \frac{\gamma^2}{1+\gamma^2}; \quad \mathrm{H} = \frac{1}{1+\gamma^2};$$

$$Q(x,y) = \left[\frac{\pi}{2\boldsymbol{K}(\mathrm{H})}\right]^{1/2}\sum_{n=0}^{\infty}\{\mathrm{e}^{-n\alpha}\Phi[(\beta(n+2\upsilon)]^{1/2}\};$$

$$\alpha = \pi\frac{\boldsymbol{K}(\Gamma) - \boldsymbol{E}(\Gamma)}{\boldsymbol{E}(\mathrm{H})}; \quad \beta = \frac{\pi^2}{\boldsymbol{K}(\mathrm{H})\boldsymbol{E}(\mathrm{H})};$$

$$x = \frac{2}{\pi}\frac{U_i}{\hbar\omega_0}\frac{\boldsymbol{E}(\mathrm{H})}{\sqrt{\Gamma}}; \quad \upsilon = \mathrm{Int}\langle x + 1\rangle - x;$$

$$\Phi(z) = \int_0^z \exp(y^2 - z^2)\mathrm{d}y.$$

Here, the operator $\mathrm{Int}\langle x + 1\rangle$ is the integer of the expression in angle brackets; $\boldsymbol{K}$ and $\boldsymbol{E}$ are the complete elliptic integrals of the first and second kinds, respectively.

The self-consistent set of equations (1)–(3) was solved by using a numerical scheme developed by the authors. The computer model was tested by performing a number of simulations of known experiments [1, 5, 7, 12]. The results of our numerical simulations were in good agreement with these experimental data. For example, we calculated a continuum generated by a 140-fs pulse in fused silica (the model of experiment [1]). This spectrum presented in Fig. 1 is asymmetric, having the extended high-frequency wing, whereas the low-frequency wing is almost absent, in accordance with experimental data [1].

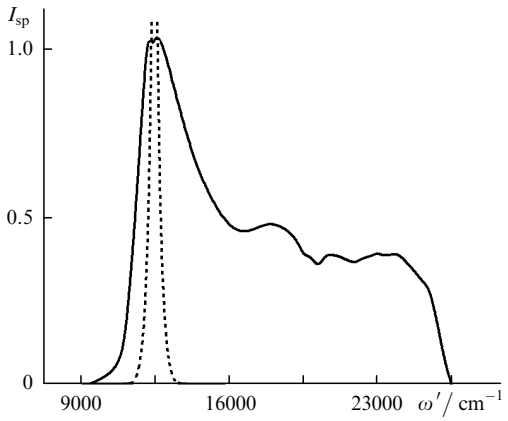

Figure 1. High-frequency continuum (solid curve) generated by a 140-fs pulse in fused silica for $P_{in}/P_{cr} = 1.1$, $\omega' = 1/\lambda$, and $\omega'_0 = 12500$ cm^{-1}; I_{sp} is normalised to the continuum maximum (dotted curve is the initial laser pulse spectrum).

3. Results of numerical experiments

We studied numerically the dynamics of the spatiotemporal intensity profile of a superpower ultrashort pulse propagating in fused silica and the evolution of its spectrum. By performing computer simulations, we found the spatiotemporal profile of a pulsed beam and determined its main parameters, in particular, spectral characteristics at any point of its propagation path in the dielectric. We used in numerical calculations the parameters of fused silica and the parameters of superpower laser radiation corresponding to real possibilities of modern lasers. It was assumed that a fused silica sample was irradiated by a Gaussian pulse with the electric field envelope

$$E(r,0,t) = E_0 \exp\left(-\frac{r^2}{w_0^2} - \frac{t^2}{\tau_p^2}\right),$$

where $I_0 = |E_0|^2$ is the initial maximum intensity; $P_{in} = \pi I_0 w_0^2$; w_0 is the initial beam width; and τ_p is the pulse duration.

Consider the most interesting results of the study. Let us discuss in more detail the evolution of an ultrashort pulse with $w_0 = 30$ μm in fused silica when the incident pulse power considerably exceeds the critical self-focusing power ($P_{in}/P_{cr} = 30$). Such a pulse propagating in fused silica experiences self-focusing. Self-focusing causes a drastic increase in the steepness of pulse leading edge. At the same time, the electron plasma density drastically increases owing to the energy imparted to electrons by the laser pulse due to ionisation [20, 21]. The contribution of defocusing in the electron plasma quite rapidly increases and begins to compete with the contribution from self-focusing.

As a result, laser radiation propagates under conditions of the dynamic competition between alternately dominating focusing and defocusing forces, resulting in the alternation of focusing and defocusing phases. The shape of the spatiotemporal envelope of the pulsed beam noticeably changes in this case. The pulsed beam propagating under such conditions, having lost more than 40 % of its initial energy, splits into tree subpulses (Fig. 2a), each of them, except the first one, propagating in a dielectric medium ionised by the previous subpulse (or subpulses). The first subpulse propagating in the glass is focused further. The peak intensity of the second subpulse propagating at a small distance from the first one and located in a strong FEP field produced by the first subpulse, decreases during the pulse propagation. At the same time, the intensity of the third subpulse, which propagates at a grater distance from the first one than the second subpulse and, therefore, is located in the FEP of lower density, also increases to rather high values (Fig. 2b). The increase in the pulsed beam intensity is accompanied by its compression and self-focusing. Due to dynamic competition between self-focusing and defocusing, the spatiotemporal envelope of the pulse intensity gradually acquires a specific shape (Fig. 3), which is preserved during some time.

One can see that the greater part of the laser pulse energy is localised in two filaments. It is very interesting that until the spatiotemporal envelope of the pulse intensity preserves its specific shape, the propagation of the pulsed beam is accompanied by a drastic broadening of the pulse spectrum. The so-called supercontinuum produced in such a way is demonstrated in Fig. 4. Note here that, unlike the continuum shown in Fig. 1, the broadenings of the spectrum in the low- and high-frequency regions are comparable (spectra similar to that shown in Fig. 1 were already observed in fused silica). After the deformation of the specific spatiotemporal envelope of the pulse intensity, the pulse spectrum decomposed into separate fragments.

Figure 4 (dashed curve) shows a supercontinuum generated by a 160-fs pulse in fused silica ($P_{in}/P_{cr} = 30$). When the laser pulse duration was decreased to 50 fs, the super-

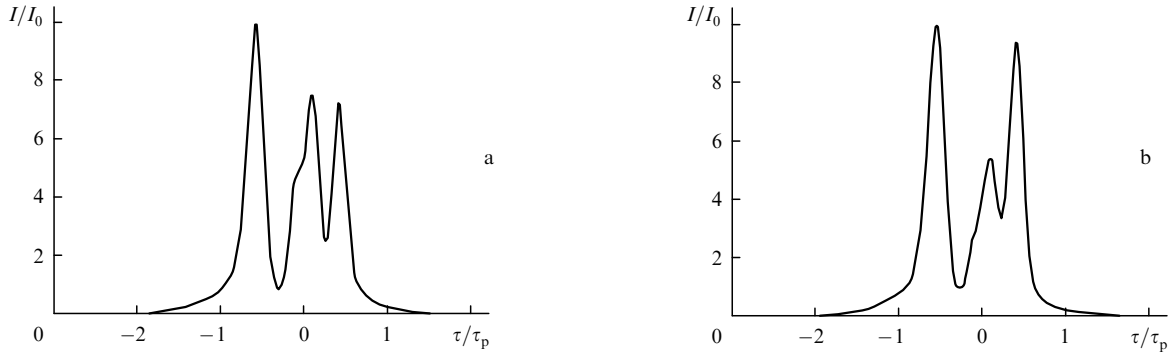

Figure 2. Temporal profile of the intensity envelope at the beam centre at distances $\zeta = 0.19$ (a) and 0.25 (b) (longitudinal coordinate $\zeta = z/L_{dif}$, $L_{dif} = 5267$ μm, $w_0 = 30$ μm, $\tau_p = 50$ fs).

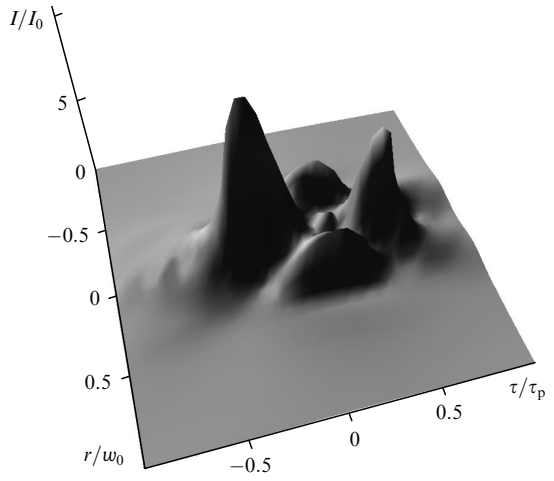

Figure 3. Spatiotemporal profile of the intensity envelope at the distance $\eta = 0.295$ (longitudinal coordinate $\zeta = z/L_{dif}$, $L_{dif} = 5267$ μm, $w_0 = 30$ μm, $\tau_p = 50$ fs, $P_{in}/P_{cr} = 30$).

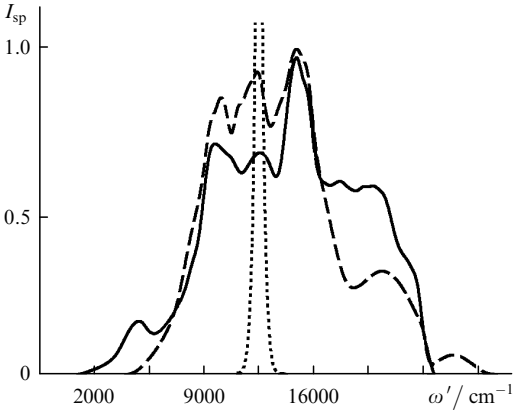

Figure 4. Supercontinuum generated by 50-fs (solid curve) and 160-fs (dashed curve) laser pulses in fused silica for $P_{in}/P_{cr} = 30$ ($\omega' = 1/\lambda, \omega'_0 = 12500\ cm^{-1}$, I_{sp} is normalised to the continuum maximum); the dotted curve is the initial spectrum.

continuum broadened somewhat and its shape became smoother (solid curve). Also, the interval along the longitudinal axis z, in which a drastic broadening of the laser pulse was observed, increased.

The supercontinuum broadening was maximal at the central part of the beam and decreased at the beam periphery. Thus, at a distance of $w_0/3$ from the beam centre, the spectrum was almost not broadened. An increase in the input power P_{in} is accompanied by a decrease in the interval along the z axis in which the supercontinuum was generated, and for $P_{in}/P_{cr} \approx 50$, the supercontinuum was not generated in fused silica in the range of parameters under study.

4. Analysis of the results

It is known that a supercontinuum is generated upon filamentation of femtosecond laser pulses in a continuous transparent medium due to self-phase modulation of a light field localised in space and time. The frequency spectrum strongly broadens due to the appearance of the time gradient of the phase [4]. The frequency shift of radiation at each spatiotemporal point is determined by the value of the time gradient of the phase φ_{nl}:

$$\Delta\omega(r,\tau) = \frac{\partial\varphi_{nl}(r,\tau)}{\partial\tau}.$$

The rate of changing phase modulation and, therefore, the broadening of the laser emission spectrum in a dielectric crystal are determined by the induced change in the refractive index Δn, which depends to a great extent on the spatiotemporal profile of a pulsed beam, in particular, on the steepness of pulse edges. The broadening of the pulsed-beam spectrum in the low-frequency region is determined by the phase growth rate at the leading edge of the pulse, i.e. by the edge steepness (the greater is the steepness, the faster the phase φ_{nl} changes and the greater is the low-frequency broadening of the spectrum), while the broadening of the spectrum in the high-frequency region is determined by the steepness of pulse trailing edge.

This explains why a continuum is generated in dielectrics, as a rule, in the high-frequency region, while the low-frequency broadening is almost absent. The matter is that the broadening of the spectrum due to the phase jump caused by the existing steepness of pulse leading edge proves to be very small. If the pulsed beam is separated into two or several beams, they propagate close to each other as the unit energy structure, and the broadening of their spectrum is caused by the steepness of the leading edge of the first subpulse and the trailing edge of the second subpulse. The phase change in the trailing edge of the pulse is mainly caused by induced ionisation processes, and here φ_{nl} decreases by several times faster (for $\tau_{f^-} \approx 1.5$ fs) than it was increased, and the phase change rate is sufficient for generating a high-frequency continuum.

After propagation of a superpower ultrashort pulse ($P_{in}/P_{cr} > 10$) through a dielectric in the regime of dynamic competition between nonlinear and ionisation processes, its spatiotemporal profile can take a specific shape: the pulse splits in the central part of the beam, unlike periphery, into two subpulses (filaments) (Fig. 3). The tail subpulse is located at such a distance from previous pulses that the effect of the FEP is insufficient for defocusing and therefore this pulse makes a considerable contribution to continuum generation in fused silica. The deformation of the spatiotemporal profile of the laser pulse is qualitatively similar to the filamentation of high-power laser radiation in air, which is also accompanied in some cases by supercontinuum generation [11].

Thus, the leading edge of the first subpulse propagates in a neutral medium and the increase in phase, which is caused to a great extent by self-focusing, occurs here comparatively slowly (according to our calculations, φ_{nl} increases with τ_p on average for 10 – 35 fs), in contrast to the trailing edge, where the phase change is caused by photoionisation processes and φ_{nl} decreases approximately for 1.5 fs. The frequency spectrum generated by this filament is presented in Fig. 5a. One can see that the spectrum is broadened in the high-frequency region, whereas the spectral broadening in the low-frequency is almost absent.

The trail subpulse is formed due to the interaction of high-power laser radiation with the dielectric and electron plasma and propagates in the field of the first subpulse; therefore, ionisation processes play a key role in the

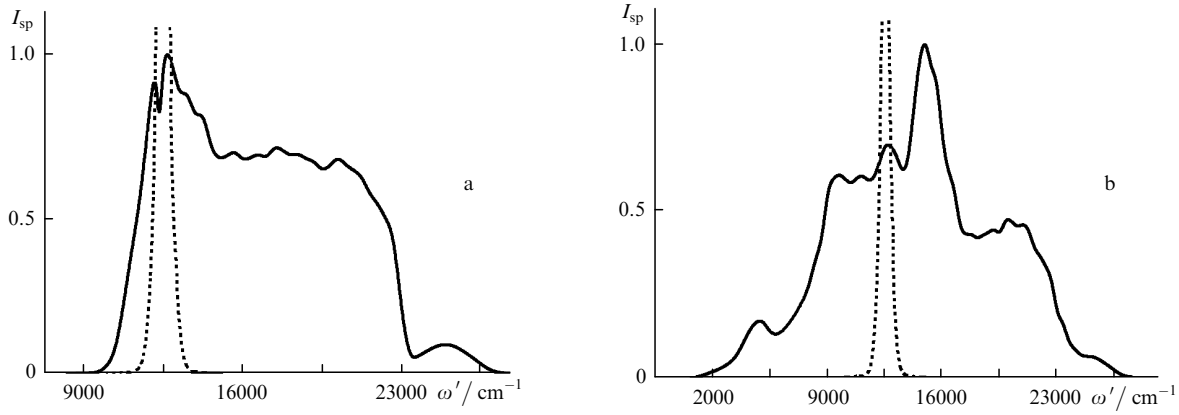

Figure 5. Continuum spectrum generated by the first (a) and second (b) axial filaments formed during the propagation of a superpower ultrashort pulse in fused silica ($P_{in}/P_{cr} = 30$, $\tau_p = 50$ fs, $w_0 = 30$ μm, $\omega'_0 = 12500$ cm^{-1}, $\omega' = 1/\lambda$). Other notation as in Fig. 4.

formation of its leading and trailing edges (for the trailing edge $\tau_{f^+} \approx \tau_{f^-} \approx 1.5 - 3$ fs). As a result, the spectrum of this filament broadens both in the high- and low-frequency regions (Fig. 5b).

It is due to a large steepness of the leading edge of the last subpulse that we observe in Fig. 4 the broadening of the laser pulse in the low-frequency region, resulting in supercontinuum generation.

Note also that supercontinuum was obtained only when we took into account in calculations the fifth-order nonlinearity and tunnelling and avalanche ionisations. For example, calculations considering the contribution of ionisation processes only due to multiphoton ionisation gave continuum spectra broadened only in the high-frequency region. It is also known that a weak normal group velocity dispersion ($\beta_d = 361$ fs^2 cm^{-1} for $\lambda = 800$ nm in fused silica) stabilises the propagation of a high-power ultrashort pulse in a dielectric [22, 23].

As a result, due to dynamic competition between nonlinear and ionisation effects, a superpower pulsed beam acquires a stable enough spatiotemporal structure (Fig. 3) in which a supercontinuum is generated.

An increase in P_{in} leads to a drastic increase in the peak intensity and the FEP density up to critical values. A comparative analysis of calculations, performed taking into account only multiphoton ionisation, with calculations taking into account the three main mechanisms (multiphoton and avalanche ionisations and tunnelling effect) showed that the radiation continuum is generated due to ionisation processes induced by intense laser pulses propagating in the dielectric crystal.

The maximum achieved FEP density remained lower than the critical density above which irreversible changes occur in the dielectric crystal [17].

5. Conclusions

We have studied some features of the propagation of superpower ($P_{in}/P_{cr} > 10$) femtosecond pulses in fused silica in the case of dynamic competition by self-focusing and defocusing caused by photoionisation.

It has been shown that for $P_{in}/P_{cr} \approx 30$ and certain parameters, a supercontinuum can be generated in fused silica, when the pulse spectrum is broadened both in the high- and low-frequency regions (to our knowledge, continuum generation was earlier observed in fused silica only in the high-frequency region). We have found that the low-frequency broadening of the 50-fs laser pulse was larger than that of the 160-fs pulse.

We have analysed the physical nature of a supercontinuum, in particular, the relation between the evolution of the spatiotemporal envelope of the laser beam intensity in fused silica and the spectrum generated by the pulse. The pulse is broadened because the pulsed beam propagating in fused silica is deformed in a certain way due to ionisation processes.

Acknowledgements. This work was supported by Grant No. NSh-4870.2006.2 of the President of the Russian Federation for Support of Leading Scientific Schools and the Russian Foundation for Basic Research (Grant No. 06-02-16801).

References

1. Brodeur A., Chin S.L. *J. Opt. Soc. Am. B*, **16** (4), 637 (1999).
2. Alfano R.R., Shapiro S.L. *Phys. Rev. Lett.*, **24**, 584 (1970).
3. Hagen C.L. et al. *IEEE Photon. Technol. Lett.*, **18** (1), 91 (2006).
4. Kandidov V.P., Kosareva O.G., Golubtsov I.S., et al. *Appl. Phys. B*, **77**, 149 (2003).
5. Dharmadhikari A.K. et al. *Opt. Express*, **12**, 695 (2004).
6. Midorikava K., Kawano H., Suda A., Nagura C., Obara M. *Phys. Rev. Lett.*, **80**, 923 (2004).
7. Dharmadhikari A.K., Rajgara F.A., Mathur D. *Appl. Phys. B,* **80**, 61 (2005).
8. Fedotova O.M., Khasanov O.Kh., Gusakov A., Hermann I. *Trudy X Vserossiiskoi shkoly-seminara 'Fizika i primenenie mikrovoln'* (Proceedings of X All-Russian Seminar on Physics and Applications of Microwaves) (Moscow: Moscow State University, 2005) p. 49.
9. Kebin Shi, Peng Li, Shizhuo Yin, Zhiwen Liu. *Opt. Express*, **12** (6), 2096 (2004).
10. Fedotov A.B., Naumov A.N., et al. *IEEE J. Sel. Top. Quantum Electron.*, **8** (3), 665 (2002).
11. Zheltikov A.M. *Usp. Fiz. Nauk*, **6**, 6 (2006).
12. Saliminia A., Chin S.L., Vallée R. *Opt. Express*, **13** (15), 5731 (2005).
13. Tzortzakis S. et al. *Opt. Commun.*, **197**, 131 (2001).
14. Tzortzakis S., Sudrie L., Franco M., Prade B., Myzyrowicz A. *Phys. Rev. Lett.*, **87**, 1 (2001).
15. Gaeta A.L. P*hys. Rev. Lett.*, **84**, 3582 (2000).
16. Sudrie L. et al. *Phys. Rev. Lett.*, **89** (18), 186601-1 (2002).
17. Couairon A. et al. *Phys. Rev. Lett.*, **71** (12), 125435-1 (2005).

18. Stuart B.C. et al. *Phys. Rev. B*, **53**, 1749 (1996).
19. Keldysh L.V. *Zh. Eksp. Teor. Fiz.*, **47**, 1945 (1964).
20. Klesik M., Katona G., Moloney J.V., Wright E.M. *Phys. Rev. Lett.*, **91**, 043905 (2003).
21. Rayner D.M., Naumov A., Corkum P.B. *Opt. Express*, **13** (9), 3208 (2005).
22. Vislobokov N.Yu. *Kvantovaya Elektron.*, **36**, 773 (2006) [*Quantum Electron.*, **36**, 773 (2006)].
23. Vislobokov N.Yu., Sukhorukov A.P., Khasanov O.Kh., Smirnova T.V., Fedotova O.M. *Mater. VI Mezhdunarodn. konf. 'Lazernaya fizika i opticheskie tekhnologii'* (Proceeding of VI International Conference on Laser Physics and Optical Technologies) (Grodno, Belarus', 2006) Pt. 2, p. 21.